Research and Reviews in Materials Science and Chemistry
Vol. 1, Issue 1, 2012, Pages 59-74
ISSN 2319-6920
Pubished Online on October 29, 2012

http://jyotiacademicpress.net

THERMOELECTRIC PROPERTIES OF *p*-TYPE $Bi_2Se_{3x}Te_{3(1-x)}$ ALLOYS PREPARED USING SOLID-STATE MICROWAVE SYNTHESIS

AREJ KADHIM, ARSHAD HMOOD and HASLAN ABU HASSAN

School of Physics
Universiti Sains Malaysia
11800, Pulau Penang
Malaysia
e-mail: areejkadhim@yahoo.com

Abstract

In the present study, thermoelectric materials based on *p*-type Bi_2Te_3 and dispersed with x compositions of selenium (Se) (x = 0.0, 0.2, 0.4, 0.6, 0.8, and 1.0) in $Bi_2Se_{3x}Te_{3(1-x)}$ ingots were prepared by using standard solid-state microwave synthesis procedures. The microstructures of the ingots were characterized by field emission scanning electron microscopy. The crystalline of the powders were examined by X-ray diffraction, which showed the formation of a rhombohedral structure. The electrical transport properties of the samples were studied from room temperature up to 500K. The results indicate that the hole concentration gradually increases, resulting in an increase in electrical conductivity and a decrease in the Seebeck coefficient with increasing Se content. The thermoelectric power factor was enhanced to $4.19 mW/mK^2$ for the sample with x = 0.2.

Keywords and phrases: chalcogenides, inorganic compounds, X-ray diffraction, electrical properties.

Communicated by Noshin Omar.

Received July 19, 2012

1. Introduction

Narrow-gap binary chalcogenides, such as Bi_2Te_3 and Bi_2Se_3, are well known as thermoelectric materials (TEs) used in a thermoelectric generator, which functions at room temperature (300K) [1-3]. The crystal structures of these chalcogenides are rhombohedral, with the space group $D_{3d}^{S}(R\bar{3}m)$. These crystal structures can be represented as a stack of hexagonally arranged atomic planes, each consisting of only one type of atom. Five atomic planes are stacked in a closely packed manner, with a $Te^{I}(Se)^{I}$-Bi-$Te^{II}(Se)^{II}$-Bi-$Te^{I}(Se)^{I}$ arrangement [4, 5]. The Bi and Te(Se) layers have been shown to be held together by strong covalent bonds, but the Te(Se)-Te(Se) layers are bonded by a weak van der Waals force. As a result, the energy of a broken covalent bond is significantly higher than that of a dangling van der Waals bond. Therefore, a Bi_2Te_3 crystal grows faster in the *a*-axis than in the *c*-axis [6, 7]. These complex crystal structures and the disordered atomic distributions of Bi_2Te_3 and Bi_2Se_3, which yield exceptionally low lattice thermal conductivity, significantly contribute to their excellent TE properties [8]. TE properties convert thermal energy directly into electrical energy or vice versa, as in power generation or refrigeration. The efficiency of a TE material is conventionally defined by its dimensionless figure of merit (ZT), where $ZT = \sigma S^2 T/k$, where T, S, σ, and k are the absolute temperature, Seebeck coefficient, electrical conductivity, and thermal conductivity, respectively.

A good TE material should have a perfect combination of high power factor (σS^2) and low thermal conductivity. ZT is very sensitive to variations in composition, suggesting that ZT could be improved by decreasing the lattice thermal conductivity with enhanced phonon scattering attributable to the lattice distortion [9-11]. Bi_2Te_3-based alloys can be good candidates for power generation applications at a

temperature range of 300K to 500K [12, 13]. To date, numerous methods have been used to prepare Bi_2Te_3-based alloys as crystals [14-16], polycrystals [17, 18], thin films [19, 20], and nanowires [21, 22]. Several techniques have been developed for the preparation of Bi_2Te_3 and Bi_2Se_3, including zone melting [23, 24], spark-plasma sintering [25-27], hot-pressed methods [28-31], and solid-state microwave synthesis [32, 33].

Solid-state microwave synthesis was recently demonstrated to be a simple, fast, energy-efficient, and environmentally friendly technique. Microwave radiations (2.45GHz) are coherent, polarized, and are capable of coupling with atomic materials, resulting in the rapid heating of such materials [34]. Furthermore, the fast synthesis is ascribed to the microwave volumetric nature of microwave heating [35]. The samples prepared by using microwaves have demonstrated an absence of solvent waste, high density, and different morphologies and microstructures in the resulting products [36-38]. In the current study, inorganic materials, such as Bi_2Te_3 and Bi_2Se_3 were identified to absorb microwaves, thus developing convenient high-yield syntheses of the polycrystalline ternary compounds $Bi_2Se_{3x}Te_{3(1-x)}$ within 10 min at 2.45GHz and 800W. The structure at 300K and the TE properties at elevated temperatures (303K to 523K) of $Bi_2Se_{3x}Te_{3(1-x)}$ (x = 0.0, 0.2, 0.4, 0.6, 0.8, and 1.0) were studied subsequently.

2. Experimental

The bismuth (Bi), tellurium (Te), and selenium (Se) used in the present research were of high purity (99.999%). All elements were weighed based on the formula $Bi_2Se_{3x}Te_{3(1-x)}$ (x = 0.0, 0.2, 0.4, 0.6, 0.8, and 1.0). Bi_2Te_3 was prepared by using a mixture of Bi (1.0439g) and Te (0.9561g), whereas Bi_2Se_3 was prepared by using a mixture of Bi (1.2765g) and Se (0.7235g) at a molar ratio of 2 : 3. The $Bi_2Se_{3x}Te_{3(1-x)}$

ingots were prepared by using a solid-state microwave synthesis reported previously [33]. Bright, whitish-blue flashes were observed emerging from the ampoule within 1 min of microwave exposure. The ingots were retrieved from the ampoule in sponge form. A Leo-Supra 50VP field emission scanning electron microscope (FESEM) (Carl Zeiss, Germany) was employed. The X-ray diffraction (XRD) patterns of the resultant powders were recorded by using an X-ray diffractometer system (PANalytical X'Pert PRO MRD PW3040) with CuKα radiation. The $Bi_2Se_{3x}Te_{3(1-x)}$ ingots were then ground before being pressed into disk shapes (diameter, 13mm; thickness, 0.5mm) by cold-pressing at 10 tons. The densities of the disks were measured by using the Archimedes method. The electrical conductivity measurements as a function of temperature (300K to 523K) were performed on all samples at a constant current (20mA) by using the four-point probe method under 10^{-3} mbar, whereas the Hall coefficient was determined at 300K with an applied magnetic field of 1T, using a Lake Shore 637 electromagnetic power supply (Lake Shore Cryotronics, Inc., USA). The Seebeck coefficient was determined by the slope of the linear relationship between the thermoelectromotive force and the temperature difference between the two ends of each sample. The voltages were recorded by using a Keithley 191 multimeter (Keithley Instruments, Inc., USA). A K-type E© Sun (ECS820C) thermocouple was used to measure the working temperature. The electrical conductivity and Seebeck coefficient were investigated for the disks at a temperature range of 300K to 500K.

3. Results and Discussion

$Bi_2Se_{3x}Te_{3(1-x)}$ ingots were produced via solid-state microwave synthesis, as shown by the FESEM images in Figure 1. The surface of the ingots suggests that the morphology changed from a non-uniform grain-sized distribution (x = 0.0) to a layered shape (x = 0.2 to 1.0). Upon the addition of Se, the FESEM observations revealed the appearance of a

typical layered and well-packed structure, which agree with the high relative densities (94%), and indicating that Se alloying is an effective approach for crystalline refinement.

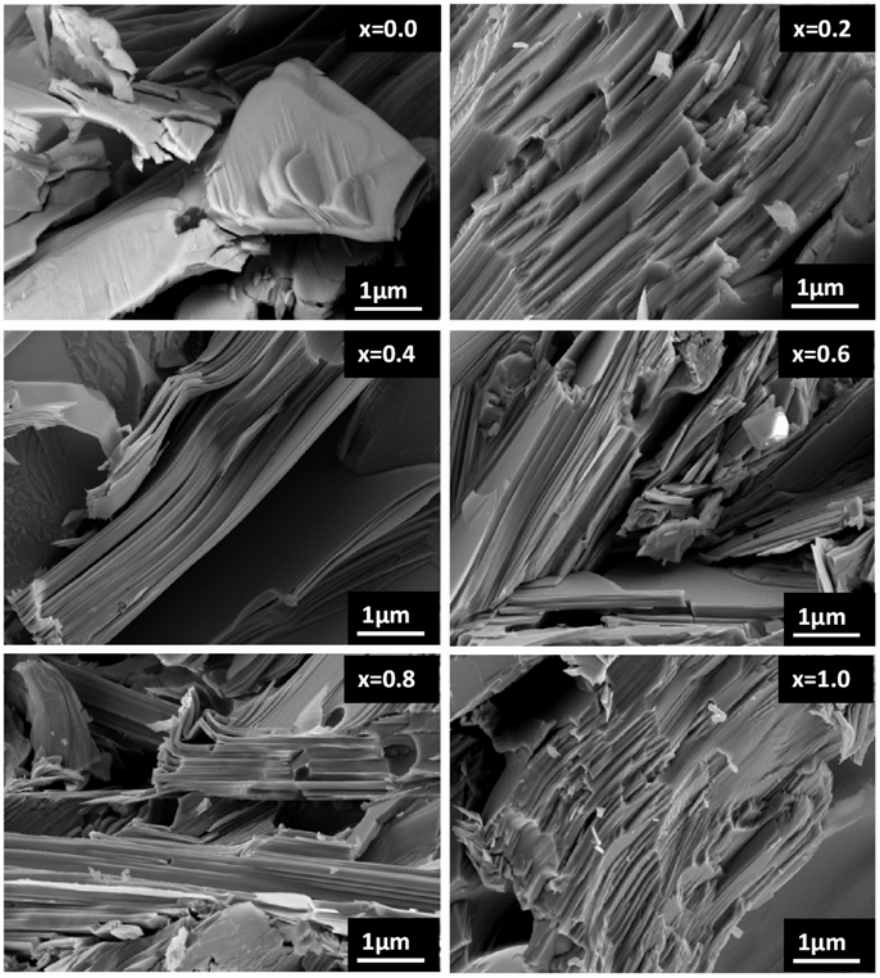

Figure 1. FESEM images of the $Bi_2Se_{3x}Te_{3(1-x)}$ ingots.

The XRD spectra illustrated in Figure 2 for the $Bi_2Se_{3x}Te_{3(1-x)}$ powders indicate that these substances are polycrystalline and characterized by a rhombohedral structure (space group $R\bar{3}m$), with a

dominant peak representing the plane (0 1 5). These results are in good agreement with the values determined by the Joint Committee on Powder Diffraction Standards for Bi_2Te_3 and Bi_2Se_3 (Card No. 15-0863 and 33-0214). No remarkable diffractions of other phases can be found, indicating that pure Bi_2Te_3 and Bi_2Se_3 were obtained.

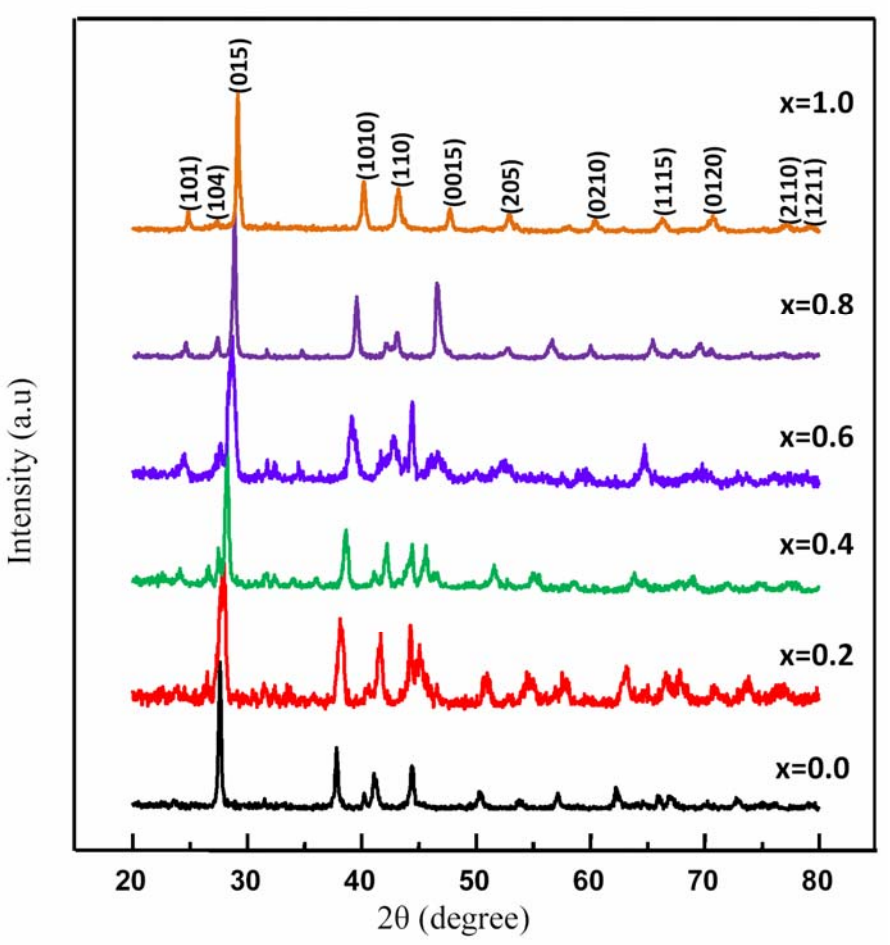

Figure 2. X-ray diffraction patterns of the $Bi_2Se_{3x}Te_{3(1-x)}$ powders prepared using rapid solid-state microwave synthesis.

The rhombohedral crystal structure can be represented as a stack of hexagonally arranged atomic planes. The lattice constant of the rhombohedral unit cell $a(R)$ for the powders can be determined by using the following relationship [39]:

$$a(R) = \frac{1}{3}\sqrt{3a(H)^2 + c(H)^2}, \tag{1}$$

where $a(H)$ and $c(H)$ are the lattice constants for the hexagonal phase structure. These lattice constants can be calculated by using the following equation [39]:

$$\frac{1}{d^2} = \frac{4}{3}\left(\frac{h^2 + hk + k^2}{a(H)^2}\right) + \frac{l^2}{c(H)^2}. \tag{2}$$

As provided in Table 1, if Se is fully substituted for Te in the whole composition range, the lattice parameters should be monotonically decreased with increasing composition and should display an apparent shift in plane (0 1 5) to the high angle (27.64º to 29.35º) with increasing Se content. The calculated $a(H)$ and $c(H)$ decrease from 4.396Å and 30.43Å for Bi_2Te_3 to 4.177Å and 28.63Å for Bi_2Se_3, respectively, whereas the lattice constant of the rhombohedral unit cell $a(R)$ decreases from 10.456Å for Bi_2Te_3 to 9.843Å for Bi_2Se_3, which is attributed to the substitution of Se $(\sim 1.15\text{Å})$ by the larger atomic radius of Te $(\sim 1.40\text{Å})$. From these results, the solid-state microwave synthesis provides a reasonable indication that the Se atoms successfully enter into the crystal lattices of Bi_2Te_3 to form the ternary compound $Bi_2Se_{3x}Te_{3(1-x)}$.

Table 1. Hexagonal lattice constants $a(H)$, $c(H)$, and rhombohedral lattice constant $a(R)$ of the $Bi_2Se_{3x}Te_{3(1-x)}$ powders obtained through XRD analysis

x	$a(H)$ (Å)	$c(H)$ (Å)	$a(R)$ (Å)
0.0	4.396	30.43	10.456
0.2	4.334	30.16	10.360
0.4	4.293	30.10	10.335
0.6	4.235	29.28	10.062
0.8	4.195	29.21	10.033
1.0	4.177	28.63	9.843

Figure 3 shows electrical conductivity as a function of temperature for the $Bi_2Se_{3x}Te_{3(1-x)}$ disks. The electrical conductivity σ of all the samples decreases with increasing temperature, exhibiting a degenerate semiconductor conducting behaviour, which suggests that the carriers are in an extrinsic state within the temperature range. Generally, the σ value increases with the Se content, with its values increasing from 1.93×10^5 S/m to 4.05×10^5 S/m at 300K and from 9.6×10^4 S/m to 1.2×10^5 S/m at 523K with x increasing from 0.0 to 1.0, respectively. The electrical conductivity can be expressed in terms of the carrier concentration (p) using the formula $\sigma = pe\mu$. The resultant conductivity that depends on Se content is explained by the increase in the carrier concentration and Hall mobility with the Se content. The electrical conductivity of the Bi_2Se_3 sample is higher than those of the samples with x = 0.0 to 0.8. This result indicates that the electrical conductivity at a fixed measuring temperature increases with increasing Se content. This result indicates that the increasing in Se, as a composition source, is attributable to the microwave irradiation effect. Thus, the microwave irradiation technique, combined with doping, is more favourable to increasing the electrical conductivity of Bi_2Te_3.

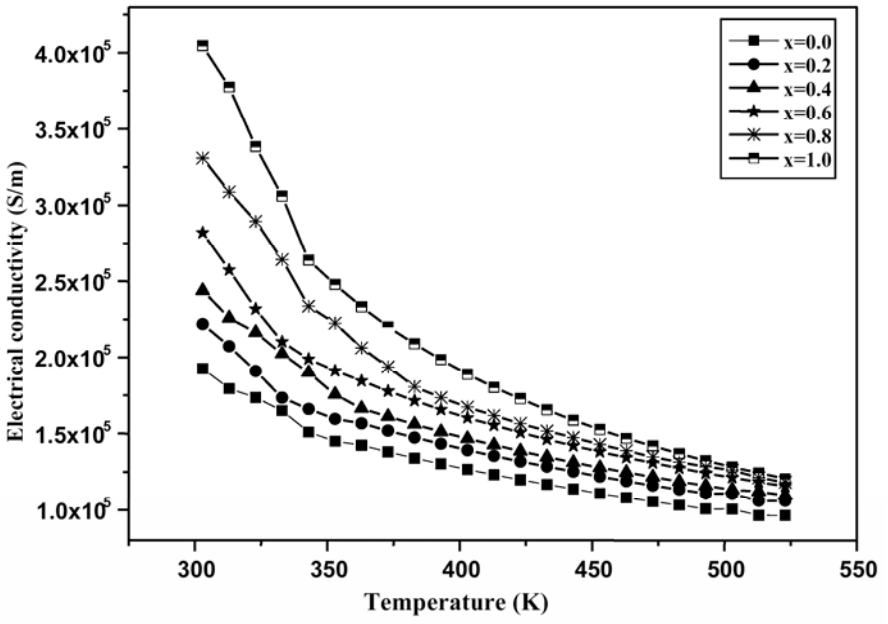

Figure 3. Electrical conductivity versus the temperature of the $Bi_2Se_{3x}Te_{3(1-x)}$ disks.

Figure 4 shows the Seebeck coefficient S as a function of the measured temperature for the $Bi_2Se_{3x}Te_{3(1-x)}$ disks. The highest value of the S is 176.3μV/K at 423K for the sample with x = 0.2, which is higher than that reported previously [40]. This result confirms that the substitution of a Se atom for Te in Bi_2Te_3 can result in a possible decrease in both the carrier concentration and mobility. Conversely, the samples with high Se content (x = 0.4, 0.6, 0.8, and 1.0) exhibit a relatively lower Seebeck coefficient.

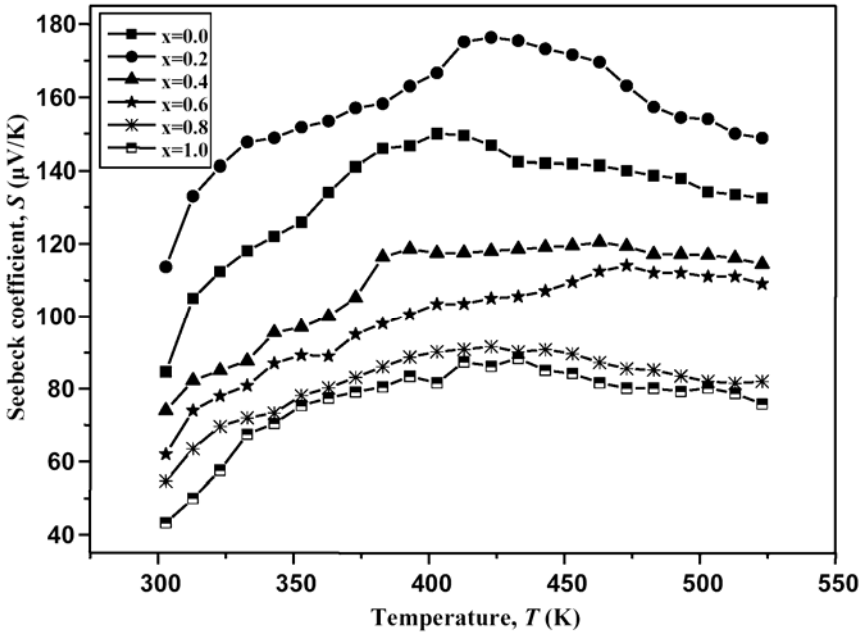

Figure 4. Seebeck coefficient versus the temperature of the $Bi_2Se_{3x}Te_{3(1-x)}$ disks.

The Seebeck coefficients of all the samples are positive (p-type), indicating that the majority of charge carriers are holes within the measuring temperature range, which agrees with the Hall effect measurement results listed in Table 2. The Hall coefficient (R_H) and electrical conductivity (σ) at room temperature were measured by using the van der Pauw method with a magnetic field strength of 1T. The corresponding carrier concentration (p) and carrier mobility (μ_H) were calculated by using the equations $p = 1/eR_H$ and $\mu_H = \sigma/pe$, respectively. Table 2 shows the dependence of the Hall mobility and carrier concentration of Bi_2Te_3 as a function of Se content. The carrier concentration of Bi_2Te_3 increases with increasing Se content. The carrier concentration for Bi_2Te_3 is $1.25 \times 10^{20}/cm^3$, slightly increasing to $1.74 \times 10^{20}/cm^3$ for Bi_2Se_3.

Table 2. Seebeck coefficient S, electrical conductivity σ, Hall coefficient R_H, carrier concentration p, and carrier mobility μ_H of the $Bi_2Se_{3x}Te_{3(1-x)}$ disks at 300K

x	$S(\mu V/K)$	$\sigma \times 10^5(S/m)$	$R_H(cm^3C^{-1})$	$p \times 10^{20}(1/cm^3)$	$\mu_H(cm^2/V.s)$
0.0	84.7	1.93	0.0500	1.25	96.50
0.2	113.7	2.22	0.0481	1.30	106.78
0.4	74.0	2.44	0.0466	1.34	113.70
0.6	62.0	2.82	0.0398	1.57	112.24
0.8	54.7	3.31	0.0369	1.69	122.14
1.0	43.3	4.05	0.0359	1.74	145.395

Based on Table 2, with the addition of Se into the binary Bi_2Te_3 compound, the carrier mobility slightly increases because of the subdued alloy scattering resulting from the further increase in the Se content [41]. Table 2 is explained by considering the dependence of the Seebeck coefficient on the carrier concentration, which can be written as follows [6]:

$$S = \frac{8\pi^2 k_B^2}{3eh^2} m^* T \left(\frac{\pi}{3p}\right)^{2/3}, \tag{3}$$

where k_B is Boltzmann's constant, h is Plank's constant, and m^* is the effective mass. The variation in the Seebeck coefficient can be understood by assuming the scattering distance of the charge carrier independent of energy and degenerate approximation [6]. The p-type nature of the Bi_2Te_3 sample can be ascribed to the increase in bond polarization energy resulting from the incorporation of more electronegative Se atoms in the Te sublattice. The substitution of Se for Te increases the Bi-chalcogen bond polarity because of the higher electronegativity value of Se (χ_{Se} = 2.4 and χ_{Te} = 2.1). Furthermore, as evidenced by quantum chemical calculations, the substitution of the Se atoms at the Te^{II} site results in a small displacement of density toward Te^{I}, whereas the

$Bi\text{-}Te^{II}$ and $Bi\text{-}Se_{Te}^{II}$ bond polarities decrease. Thus, the substitution of a more electronegative atom (with the increase in Se content) for the Te site, V_{Te}, or V_{Se} occurs, and Bi_{Te} increases slightly. Based on the experimental evidence of a reduced hole concentration and the relationship between the free carrier concentration with lattice point defects, $[V_{Te}] > [Bi_{Te}]$: p-Bi_2Te_3:$[h] = [Bi_{Te}] - [V_{Te}]$ can be assumed. Similar phenomena were also observed in previous reports [42, 43].

Figure 5 shows the power factor as a function of the measured temperature for the $Bi_2Se_{3x}Te_{3(1-x)}$ disks. The maximum power factor measured at 363K for the $Bi_2Se_{0.6}Te_{2.4}$ sample reaches $4.19 mW/mK^2$, which is larger than that reported by Wang et al. [44]. This result is ascribed to the increased Seebeck coefficient for the sample with x = 0.2. For the samples with x = 0.4 to 1.0, the power factor values decrease with rising Se composition. This result is attributed to the compounds with lower Se, which exhibit relatively better electrical properties and may be promising candidates for thermoelectric applications.

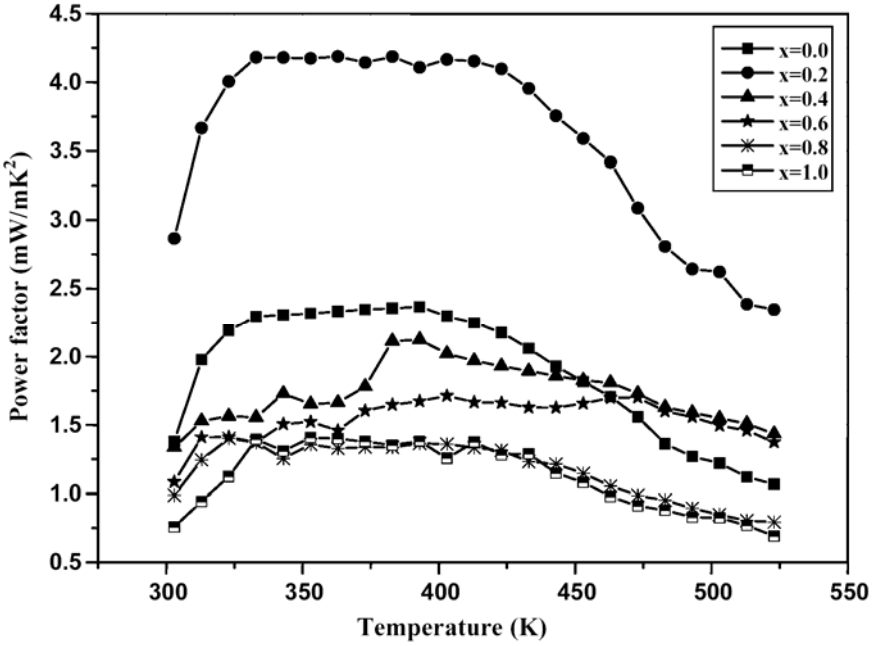

Figure 5. Power factor versus the temperature of the $Bi_2Se_{3x}Te_{3(1-x)}$ disks.

4. Conclusion

Polycrystalline $Bi_2Se_{3x}Te_{3(1-x)}$ (x = 0.0, 0.2, 0.4, 0.6, 0.8, and 1.0) samples were successfully prepared by solid-state microwave synthesis. The FESEM and XRD characterizations reveal that these products are pure Bi_2Te_3 and Bi_2Se_3 with uniform structures. The measurements of the thermoelectric properties show that the samples are degenerate *p*-type semiconductors. As a result, a maximum Seebeck coefficient of $176.3\mu V/K$ at 423K is achieved for the $Bi_2Se_{0.6}Te_{2.4}$ sample, which also shows an improved power factor. A maximum power factor value of $4.19mW/mK^2$ at 363K was obtained for the $Bi_2Se_{0.6}Te_{2.4}$ sample, whereas the values of $2.37mW/mK^2$ and $1.38mW/mK^2$ were obtained

for the Bi_2Te_3 and Bi_2Se_3 samples, respectively. This result indicates that the solid-state microwave synthesis technique is a useful tool for improving thermoelectric performance.

Acknowledgement

The authors acknowledge the partial funding provided by the PRGS Grant No. 1001/PFIZIK/844091, School of Physics, Universiti Sains Malaysia.

References

[1] S. Hong, S. Lee and B. Chun, Mater. Sci. Eng. B 98 (2003), 232-238.

[2] L. Zhao, B. Zhang, J. Li, M. Zhou, W. Liu and J. Liu, J. Alloys Comp. 455 (2008), 259-264.

[3] C. Moon, S. Shin, D. Kim and T. Kim, J. Alloys Comp. 504 (2010), S504-S507.

[4] S. Nakajima, J. Phys. Chem. Solids 24 (1963), 479-485.

[5] Y. Zhou, X. Li, S. Bai and L. Chen, J. Cryst. Growth 312 (2010), 775-780.

[6] D. H. Kim, C. Kim, S. H. Heo and H. Kim, Acta Materialia 59 (2011), 405-411.

[7] Q. Zhao and Y. G. Wang, J. Alloys Comp. 497 (2010), 57-61.

[8] Y. Zhang, G. Xu, J. Mi, F. Han, Ze. Wang and C. Ge, Mater. Res. Bull. 46 (2011), 760-764.

[9] Y. H. Zhang, T. J. Zhu, J. P. Tu and X. B. Zhao, Mater. Chem. Phys. 103 (2007), 484.

[10] T. Su, P. Zhu, H. Ma, G. Ren, L. Chen, W. Guo, Y. Iami and X. Jia, Solid State Comm. 138 (2006), 580-584.

[11] Jun Jiang, Lidong Chen, Shengqiang Bai, Qin Yao and Qun Wang, J. Cryst. Growth 277 (2005), 258-263.

[12] G. Kavei and M. A. Karami, Bull. Mater. Sci. 29 (2006), 659.

[13] K. Y. Lee and T. S. Oh, Mater. Sci. Forum 534 (2007), 1493.

[14] V. S. Zemskov, A. D. Belaya, U. S. Beluy and G. N. Kozhemyakin, J. Cryst. Growth 212 (2000), 161-166.

[15] J. Jiang, L. D. Chen, Q. Yao, S. Q. Bai and Q. Wang, Mater. Chem. Phys. 92 (2005), 39.

[16] F. Köng, Cryst. Res. Technol. 33 (1998), 219.

[17] S. J. Hong and B. S. Chun, Mater. Sci. Eng. A 356 (2003), 345-351.

[18] T. Kim and B. Chun, J. Alloys Comp. 437 (2007), 225-230.

[19] A. Li. Bassi, A. Bailini, C. S. Casari, F. Donati, A. Mantegazza, M. Passoni, V. Russo and C. E. Bottani, J. Appl. Phys. 105 (2009), 124307.

[20] J. Zhou, S. Li, H. M. A. Soliman, M. S. Toprak, M. Muhammed, D. Platzek and E. Muller, J. Alloys Comp. 471 (2009), 278-281.

[21] Y. M. Lin, O. Rabin, S. B. Cronin, J. Y. Ying and M. S. Dresselhaus, Appl. Phys. Lett. 81 (2002), 2403.

[22] K. G. Biswas, T. D. Sands, B. A. Cola and X. F. Xu, Appl. Phys. Lett. 94 (2009), 223116.

[23] O. B. Sokolov, S. Ya. Skipidarov and N. I. Duvankov, J. Cryst. Growth 236 (2002), 181-190.

[24] M. H. Ettenberg, J. R. Maddux, P. J. Taylor, W. A. Jesser and F. D. Rosi, J. Cryst. Growth 179 (1997), 495-502.

[25] D. Ilzycer, M. Sinvani, R. Dukhan, R. Weingarten and M. Shiloh, J. Cryst. Growth 87 (1988), 107-112.

[26] M. Omori, Mater. Sci. Eng. A 287 (2000), 183-188.

[27] X. A. Fan, J. Y. Yang, W. Zhu, H. S. Yun, R. G. Chen, S. Q. Bao and X. K. Duan, J. Alloys Comp. 420 (2006), 256-259.

[28] T. S. Oh, D. B. Hyum and N. V. Kolomoets, Scr. Mater. 42 (2000), 849.

[29] T. S. Kim, I. S. Kim, T. K. Kim, S. J. Hong and B. S. Chun, Mater. Sci. Eng. B 90 (2002), 42-46.

[30] H. L. Ni, T. J. Zhu and X. B. Zhao, Mater. Sci. Eng. B 117 (2005), 119-122.

[31] X. H. Ji, X. B. Zhao, Y. H. Zhang, B. H. Lu and H. L. Ni, J. Alloys Comp. 387 (2005), 282-286.

[32] C. Mastrovito, J. W. Lekse and J. A. Aitken, J. Solid State Chem. 180 (2007), 3262-3270.

[33] A. Kadhim, A. Hmood and H. Abu Hassan, Mater. Lett. 65 (2011), 3105-3108.

[34] T. Suriwong, S. Thongtem and T. Thongtem, Mater. Lett. 63 (2009), 2103-2106.

[35] G. Zhou, V. G. Pol, O. Palchik, A. R. Kerner, E. Sominski, Y. Koltypin and A. Gedanken, J. Solid State Chem. 177 (2004), 361-365.

[36] K. J. Rao, B. Vaidhyanathan, M. Ganguli and P. A. Ramakrishnan, Chem. Mater. 11 (1999), 882.

[37] R. Roy, D. Agrawal, J. Cheng and S. Gedevanishvili, Nature 401 (1999), 304.

[38] M. Jeselnik, R. S. Varma, S. Polanc and M. Kocevar, Green Chem. 4 (2002), 35.

[39] B. D. Cullity, Element of X-Ray Diffraction, (3rd Edition), Wesley Publishing Company, USA, 1967.

[40] Fei Li, Xiangyang Huang, Zhengliang Sun, Juan Ding, Jun Jiang, Wan Jiang and Lidong Chen, J. Alloys Comp. 509 (2011), 4769-4773.

[41] X. A. Fan, J. Y. Yang, R. G. Chen, W. Zhu and S. Q. Bao, Mater. Sci. Eng. A 438-440 (2006), 190-193.

[42] S. Augustine and E. Mathai, Semicond. Sci. Tech. 18 (2003), 745-754.

[43] J. Horák, J. Navrátil and Z. Starý, J. Phys. Chem. Solids 53 (1992), 1067-1072.

[44] S. Wang, W. Xie, H. Li and X. Tang, Intermetallics 19 (2011), 1024-1031.

■